PHYSICAL REVIEW D **86,** 094028 (2012)

Nonleptonic two-body B_c-meson decays

Sk. Naimuddin,[1] Susmita Kar,[2] M. Priyadarsini,[3] N. Barik,[4] and P. C. Dash[5,*]

[1]*Physics Department, Maharishi College of Natural Law, Bhubaneswar 751007, India*
[2]*Physics Department, North Orissa University, Baripada 757003, India*
[3]*Physics Department, ITER, SOA University, Bhubaneswar 751030, India*
[4]*Retired Professor of Physics, Utkal University, Bhubaneswar 751004, India*
[5]*Physics Department, ITER, SOA University, Bhubaneswar 751030, India*

(Received 28 June 2012; revised manuscript received 23 September 2012; published 19 November 2012)

We study the exclusive nonleptonic two-body B_c decays within factorization approximation, in the framework of the relativistic independent quark model based on a confining potential in the scalar-vector harmonic form. The relevant weak form factors and branching ratios for different decay modes ($B_c \to PP, PV, VP$) are predicted in reasonable agreement with other quark model predictions. We find that the dominant contribution to the B_c-meson lifetime comes from the Cabibbo-Kobayashi-Masakawa favored $\bar{c} \to \bar{s}, \bar{d}$ decay modes, and the most promising modes are found to be $B_c^- \to \bar{B}_s^0 \pi^-$, $B_c^- \to \bar{B}_s^0 \rho^-$ and $B_c^- \to \bar{B}_s^{\star 0} \pi^-$ with predicted branching ratios of 12.01, 9.96, and 8.61%, respectively, which might be easily detected at the hadron collider in the near future.

DOI: 10.1103/PhysRevD.86.094028 PACS numbers: 13.25.Hw, 12.39.Pn

I. INTRODUCTION

The discovery of the B_c meson by the collider detector at Fermilab (CDF Collaboration) [1] in 1998 has aroused a great deal of interest in its production mechanism, spectroscopy and decay properties. Subsequent measurements of its lifetimes, τ_{B_c}, and mass, M_{B_c}, leading to the recent announcement of the CDF and DO Collaborations $\tau_{B_c} = 0.463^{+0.073}_{-0.065}$ (Stat) $\pm$ 0.036(Syst) ps [2], $M_{B_c} = 6.2756 \pm 0.0029$ (Stat) $\pm$ 0.0026(Syst) GeV [2] and $M_{B_c} = 6.3 \pm 0.014$ (Stat) $\pm$ 0.005(Syst) GeV [3] have opened new windows for analysis of heavy quark dynamics. The LHC is expected to produce around 5×10^{10} B_c events per year which would provide important clues to study decay properties and test standard model predictions in this sector.

The B_c meson decays are of theoretical interest due to its characteristic special features: (1) Being the lowest bound state of two different heavy quarks with open flavors (b and c), it cannot annihilate into gluons and is stable against strong and electromagnetic interactions. The B_c meson, therefore, decays via weak interaction. (2) Both its constituents being heavy, each of these can decay individually, yielding rich decay channels. The tree- level weak decay of the B_c meson can be broadly divided into three categories: (i) $b \to q$ (q = c, u)-induced mode with c quark as the spectator, (ii) $c \to q$ (q = s, d)-induced mode with b quark as the spectator, and (iii) the relatively suppressed weak annihilation mode. The pure leptonic B_c decays which belong to the annihilation mode can be used to measure the decay constant f_{B_c} and Cabibbo-Kobayashi-Masakawa (CKM)-matrix element $|V_{bc}|$. However, these decays cannot be fully reconstructed due to the missing neutrino. Of the other two categories of B_c-meson decays, one naively expects $c \to q$ transition to be kinematically suppressed compared to $b \to q$ transitions on grounds of available phase space alone ($m_c^5 \ll m_b^5$). However, the CKM-matrix elements involved are greatly in favor of the former ($V_{cb} \ll V_{cs}$), which overcompensates its kinematic suppression. The estimates [4] show that the dominant contribution of about 70% to the B_c lifetime comes from $c \to q$ transitions, where $b \to q$ transitions and the weak annihilation barely contribute about 20% and 10%, respectively. Thus, the decay rates for the former two categories of B_c decays are competitive in magnitude.

There have been several theoretical studies [4–36] on semileptonic and nonleptonic B_c-meson decays. The semileptonic B_c decays provide an excellent laboratory to measure the CKM-matrix elements: V_{cb}, V_{ub}, V_{cs} and V_{cd} and the weak form factors for B_c transitions to charm and bottom mesons. These decays are easy to handle as the relevant matrix element of the quark currents is parametrized in terms of a few hadronic form factors. The description of nonleptonic decays is, however, nontrivial as these processes are strongly influenced by confining color forces and involve matrix elements of the local four quark operators, which are more complicated than the current operators of semileptonic decays. The semileptonic B_c-meson decays have been studied [36] in the relativistic independent quark model (RIQM) [37–41] based on a confining potential in the scalar-vector harmonic form, where we predict relevant form factors and their q^2 dependence in the allowed kinematic range, yielding branching ratios in reasonable agreement with the data and other model predictions.

In this paper we intend to extend the applicability of the (RIQM) model to study, within factorization approximation, the two-body exclusive nonleptonic B_c-meson decays to PP, PV and VP final states. The QCD

*purendradash@gmail.com

factorization approximation is widely used to study these decays, since it works reasonably well in the heavy-quark physics. In this approach, the hadronic matrix element of the local four quark operators is taken as a product of one-particle matrix elements which are parametrized in terms of weak form factors and decay constants. Justification of factorization approximation is based on Bjorken's intuitive argument on color transparency [42], theoretical developments on QCD approach in the $\frac{1}{N_c}$ limit [43] and heavy-quark effective theory [44] etc. As done in Refs. [5–11,45,46], we consider here the contribution of current-current operators only in predicting tree-level nonleptonic B_c-meson decays. In the evaluation of decay width, the contribution of the tree diagram is expected to be dominant. The penguin contribution may be important in evaluating CP violation and the search for new physics beyond the standard model, which we do not consider in this work. The Wilson's coefficient of the penguin operator being very small, the corresponding contributions to weak-decay amplitudes only become relevant in rare decays, where the tree-level contribution is either strongly CKM suppressed, as in $\bar{B} \to \bar{K}^{\star}\pi$, or where matrix elements of current-current operators do not contribute at all, as in $\bar{B} \to \bar{K}^{\star}\gamma$ and $\bar{B}^0 \to \bar{K}^0\phi$ [47]. In this paper we do not consider these decays. The contribution of QCD and electroweak penguin operators has also been shown [17,46] to be too tiny compared to that of current-current operators due to serious suppression of CKM elements.

The paper is organized as follows. In Sec. II we provide the general remark on the factorization hypothesis and nonleptonic decay amplitudes. In Sec. III we describe the decay amplitudes in the framework of the RIQM-model and extract the model expressions for relevant weak form factors and B_c decay width. We discuss our numerical results in Sec. IV. Section V contains the summary and conclusion.

II. FACTORIZATION AND NONLEPTONIC DECAY AMPLITUDES

In the factorization approach, the decay amplitude for the two-body nonleptonic transition $M \to m_1 m_2$ can be approximated by the product of one-particle matrix elements [5,48,49]

$$\begin{aligned}\langle m_1 m_2|\mathcal{H}_{\rm eff}|M\rangle &= \frac{G_F}{\sqrt{2}} V_{q_{1(2)}q'_{1(2)}} V_{q_3 q'_3}[a_1(\mu)\langle m_2|J^\mu|0\rangle\langle m_1|J_\mu|M\rangle \\ &\quad + a_2(\mu)\langle m_1|J^\mu|0\rangle\langle m_2|J_\mu|M\rangle],\end{aligned} \tag{1}$$

where G_F is the Fermi constant, V_{ij}'s are Cabibbo-Kobayashi-Maskawa (CKM) matrix elements, and $a_1(\mu)$ and $a_2(\mu)$ are the QCD factors expressed in terms of the Wilson's coefficients as

$$\begin{aligned}a_1(\mu) &= C_1(\mu) + \frac{1}{N_c} C_2(\mu); \\ a_2(\mu) &= C_2(\mu) + \frac{1}{N_c} C_1(\mu).\end{aligned} \tag{2}$$

Here, N_c denotes the number of colors and $J_\mu \equiv V_\mu - A_\mu \equiv \bar{q}'_{1(2)}\gamma_\mu(1-\gamma_5)q_{1(2)}$ is the vector-axial current.

In general cases, the renormalization point (μ) dependence of the product of current operator matrix elements does not cancel the μ dependence of $a_{1,2}(\mu)$. The nonfactorizable contribution to Eq. (1) must be present to make the physical amplitude renormalization scale independent. In the present analysis as in Ref. [41,49], the nonfactorizable vertex, penguin and hard-spectator corrections are thought to be incorporated into the effective Wilson's coefficients $a_i (i = 1, 2)$.

In QCD factorization, in the heavy-quark limit, and to leading order α_s, the current-current amplitude can be factorized into a product of two single quark currents if weak annihilation contributions are ignored. We neglect here the so-called W exchange and annihilation diagrams, since in the limit $M_W \to \infty$, they are connected by Fiertz transformation and are doubly suppressed by the kinematic factor of the order (m_i^2/M^2). We also discard the color octet currents which emerge after the Fiertz transformation of color-singlet operators. Clearly, these currents violate factorization since they cannot provide transitions to the vacuum states.

The nonvanishing part of the matrix elements of the current J^μ between the vacuum and final meson (pseudoscalar P/vector V) states in covariant form are parametrized by meson decay constants $f_{P,V}$

$$\begin{aligned}\langle P|\bar{q}'_3\gamma^\mu\gamma_5 q_3|0\rangle &= i f_P p_P^\mu; \\ \langle V|\bar{q}'_3\gamma^\mu q_3|0\rangle &= e^{*\mu} f_V m_V.\end{aligned} \tag{3}$$

The covariant decomposition of the nonvanishing matrix elements of the weak current J_μ between the initial and final pseudoscalar meson state is expressed in the form:

$$\begin{aligned}&\langle P(p_P)|\bar{q}'_{1(2)}\gamma_\mu q_{1(2)}|M(p)\rangle \\ &= \left[(p+p_P)_\mu - \frac{M^2-m_P^2}{q^2} q_\mu\right] F_1(q^2) \\ &\quad + \frac{M^2-m_P^2}{q^2} q_\mu F_0(q^2) \\ &= (p+p_P)_\mu f_+(q^2) + (p-p_P)_\mu f_-(q^2),\end{aligned} \tag{4}$$

where

$$f_+(q^2) = F_1(q^2), \tag{5}$$

$$f_-(q^2) = \frac{M^2-m_P^2}{q^2}[F_0(q^2) - F_1(q^2)]. \tag{6}$$

For the vector-meson final state, the corresponding matrix element is parametrized separately for vector and axial-vector parts as

$$\langle V(p_V)|\bar{q}'_{1(2)}\gamma_\mu q_{1(2)}|M(p)\rangle = \frac{2V(q^2)}{M+m_V} i\epsilon_{\mu\nu\rho\sigma} e^{\star\nu} p^\rho p_V^\sigma, \tag{7}$$

$$\begin{aligned}\langle V(p_V)|\bar{q}'_{1(2)}\gamma_\mu\gamma_5 q_{1(2)}|M(p)\rangle &= (M+m_V)e^\star_\mu A_1(q^2) - \frac{A_2(q^2)}{M+m_V}(e^\star\cdot q)(p+p_V)_\mu \\ &\quad - 2m_V\frac{e^\star\cdot q}{q^2}q_\mu A_3(q^2) + 2m_V\frac{e^\star\cdot q}{q^2}q_\mu A_0(q^2),\end{aligned} \tag{8}$$

where

$$A_3(q^2) = \frac{M+m_V}{2m_V}A_1(q^2) - \frac{M-m_V}{2m_V}A_2(q^2). \tag{9}$$

Here, we take p, $p_{P,V}$ as the four-momentum of the initial and final state meson, respectively. $q = p - p_{P,V}$ denotes the four-momentum transfer and $e^\star$, the polarization vector of the final state vector meson.

In order to cancel the poles at $q^2 = 0$, the form factors $F_1(q^2)$, $F_0(q^2)$ and $A_3(q^2)$ and $A_0(q^2)$ satisfy the necessary conditions:

$$F_1(0) = F_0(0), \qquad A_3(0) = A_0(0). \tag{10}$$

The decay width for the two-body nonleptonic transitions with two pseudoscalar mesons (P_1, P_2) in the final states is written in terms of effective decay amplitude A as

$$\Gamma(M\to P_1P_2) = \frac{|\vec{k}|}{8\pi M^2}|A(M\to P_1P_2)|^2, \tag{11}$$

where the three-momentum magnitude $|\vec{k}|$ of the final state meson in the parent meson rest frame is

$$\begin{aligned}|\vec{k}| = |\vec{p}_{P_1}| &= |\vec{p}_{P_2}| \\ &= \frac{1}{2M}\{[M^2 - (m_{P_1}+m_{P_2})^2][M^2 \\ &\quad - (m_{P_1}-m_{P_2})^2]\}^{1/2}.\end{aligned} \tag{12}$$

The corresponding expression of the decay width for $M\to PV(VP)$ with a pseudoscalar and a vector meson in the final states is written as

$$\Gamma(M\to PV, VP) = \frac{|\vec{k}|^3}{8\pi m_V^2}|A(M\to PV, VP)|^2 \tag{13}$$

with

$$|\vec{k}| = \frac{1}{2M}\{[M^2-(m_{P,V}+m_{V,P})^2][M^2-(m_{P,V}-m_{V,P})^2]\}^{1/2}. \tag{14}$$

Here, the relevant decay amplitude A is expressed in the form:

$A = \frac{G_F}{\sqrt{2}}$ (CKM factors) (QCD factor) $(M^2 - m_{P_1}^2)\times f_{P_2}F_0^{M\to P_1}(q^2)$,

$A = \frac{G_F}{\sqrt{2}}$ (CKM factors) (QCD factor) $2m_V f_V F_1^{M\to P}(q^2)$ and

$A = \frac{G_F}{\sqrt{2}}$ (CKM factors) (QCD factor) $2m_V f_P A_0^{M\to V}(q^2)$

for $M\to P_1P_2$, $M\to PV$ and $M\to VP$ decays, respectively. The standard factorization scheme shown in Eq. (1) can be used to calculate decay amplitudes in Eqs. (11) and (13) with the factorized amplitudes (1) in terms of meson decay constants (4) and weak form factors (5)–(9). The meson decay constants have been observed experimentally and also predicted in different models, which one can take as input parameters. The study of nonleptonic decays is, therefore, reduced to calculation of relevant weak form factors and their q^2 dependence in the allowed kinematical range in the framework of a suitable bound state model, such as the (RIQM) model described in the following section.

III. WEAK DECAY FORM FACTORS AND DECAY WIDTH IN THE RELATIVISTIC INDEPENDENT QUARK MODEL

We study the nonleptonic B_c decays in three separate categories with (i) two pseudoscalar mesons (P_1, P_2), (ii) a pseudoscalar and a vector meson (P, V) and (iii) a vector and a pseudoscalar meson (V, P) in the final state. The decay amplitude corresponding to each category can be calculated from the relevant tree-level Feynman diagrams shown in Fig. 1. The color-favored "class I" decays represented by the diagram [Fig. 1(a)] are characterized by external emission of W boson, where the nonvanishing factorized amplitude is proportional to the QCD factor $a_1(\mu)$. The color-suppressed transitions known as class II decays, represented by the diagram [Fig. 1(b)], are characterized by internal W emission, where the nonvanishing decay amplitude is proportional to the QCD factor $a_2(\mu)$. Figure 1(c) represents class III decays in which both the color-favored and color-suppressed diagrams contribute to the decay amplitude. In these processes, the factorized amplitudes corresponding to both the QCD factors—$a_1(\mu)$ and $a_2(\mu)$—interfere. In this section we calculate explicitly the decay amplitudes corresponding to the color-favored $M\to P_1P_2$, PV, VP transitions from the Feynman diagram shown in Fig. 1(a).

A. $M\to P_1P_2$

At the constituent level, the process $M\to P_1P_2$ can be considered as the decay of one of the constituent quarks $q_{1(2)}$ with four-momentum $p_{q_{1(2)}}$ inside the decaying meson state $|M(\vec{p}, S_M)\rangle$ to the W boson and a daughter quark/antiquark $q'_{1(2)}$ of momentum $p_{q'_{1(2)}}$ which along with the spectator $q_{2(1)}$ of momentum $p_{q_{2(1)}}$ hadronize to one of the

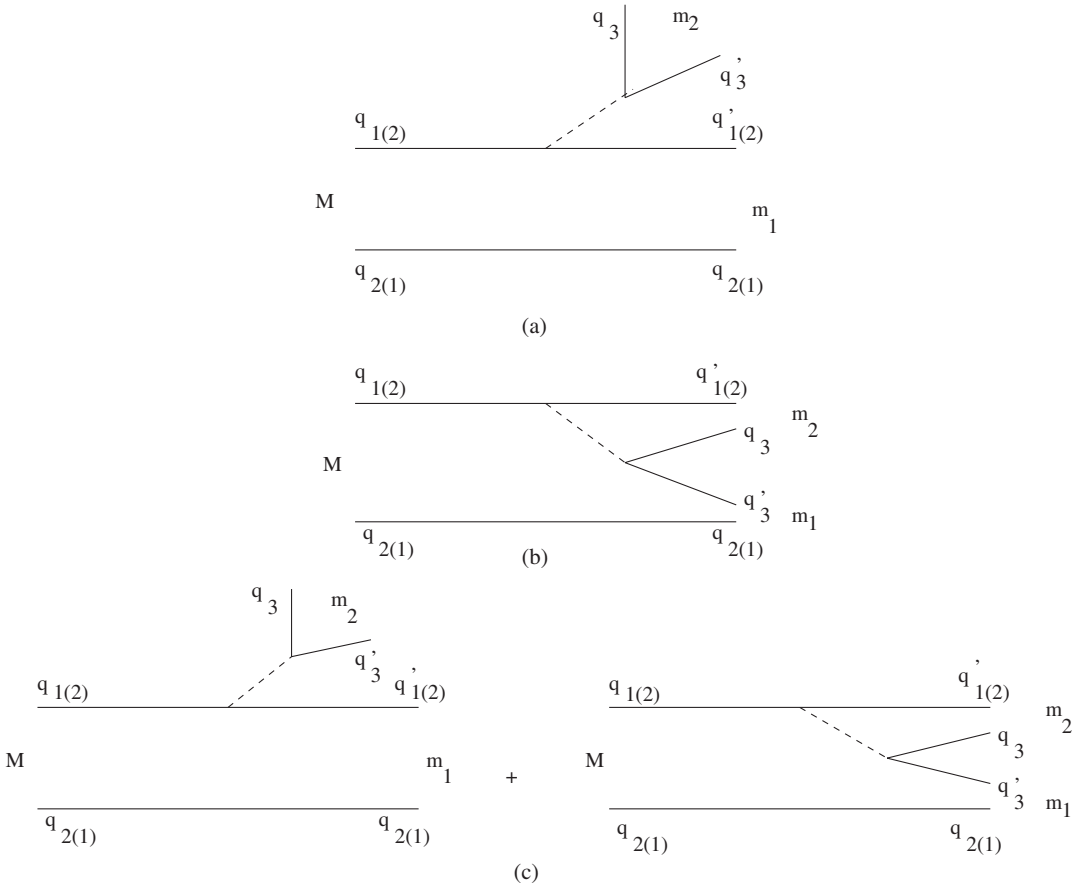

FIG. 1. Quark level diagram of nonleptonic decay of meson: $M \rightarrow m_1 m_2$.

final state mesons: $|P_1(\vec{k}, S_{P_1})\rangle$. The externally emitted W boson with four-momentum q then decays to a quark-antiquark $(q_3 q_3')$ pair which ultimately hadronize to another final meson state $|P_2(\vec{q}, S_{P_2})\rangle$. The decay, in fact, occurs physically between the momentum eigenstates of the participating mesons. Therefore, in a field theoretic treatment, the meson state should be represented by an appropriate wave packet, reflecting the momentum and spin distribution between the constituents inside the meson core. In the present model, the momentum wave packet description of the meson corresponding to a definite momentum $(\vec{p})$ and spin (S_M) state is taken in the general form [36,39–41]:

$$|M(\vec{p}, S_M)\rangle = \frac{1}{\sqrt{N_M(\vec{p})}} \sum_{\lambda_1, \lambda_2 \in S_M} \zeta^M_{q_1, \bar{q}_2}(\lambda_1, \lambda_2) \times \int d^3\vec{p}_{q_1} d^3\vec{p}_{q_2} \delta^{(3)}(\vec{p}_{q_1} + \vec{p}_{q_2} - \vec{p}) \times \mathcal{G}_M(\vec{p}_{q_1}, \vec{p}_{q_2}) \hat{b}^\dagger_{q_1}(\vec{p}_{q_1}, \lambda_1) \hat{\bar{b}}^\dagger_{q_2}(\vec{p}_{q_2}, \lambda_2) \mid 0\rangle, \tag{15}$$

where $\hat{b}^\dagger_{q_1}(\vec{p}_{q_1}, \lambda_1)$ and $\hat{\bar{b}}^\dagger_{q_2}(\vec{p}_{q_2}, \lambda_2)$ are, respectively, the quark and antiquark creation operator. $\zeta^M_{q_1, \bar{q}_2}(\lambda_1, \lambda_2)$ stands for the SU(6) spin-flavor coefficients for the meson state. $N_M(\vec{p})$ is the meson normalization realized from $\langle M(\vec{p}) \mid M(\vec{p}')\rangle = \delta^{(3)}(\vec{p} - \vec{p}')$ in the integral form:

$$N_M(\vec{p}) = \int d^3\vec{p}_{q_1} \mid \mathcal{G}_M(\vec{p}_{q_1}, \vec{p} - \vec{p}_{q_1})|^2. \tag{16}$$

Finally, $\mathcal{G}_M(\vec{p}_{q_1}, \vec{p} - \vec{p}_{q_1})$, which represents the effective momentum distribution function for the quark q_1 and antiquark $\bar{q}_2$, is taken in the form [36,39–41]

$$\mathcal{G}_M(\vec{p}_{q_1}, \vec{p} - \vec{p}_{q_1}) = \sqrt{G_{q_1}(\vec{p}_{q_1}) \tilde{G}_{\bar{q}_2}(\vec{p} - \vec{p}_{q_1})}. \tag{17}$$

Here, $G_{q_1}(\vec{p}_{q_1})$ and $\tilde{G}_{\bar{q}_2}(\vec{p} - \vec{p}_{q_1})$ refer to the momentum probability amplitude of the bound quark q_1 with momentum $\vec{p}_{q_1}$ and antiquark $\bar{q}_2$ with momentum $\vec{p} - \vec{p}_{q_1}$, respectively. The bound quark and antiquark inside the meson core are in the definite energy states with no definite momenta of their own. However, it is possible to obtain their momentum probability amplitudes via appropriate momentum space projection of the corresponding quark-antiquark eigenmodes derivable from the model. The model expression for $G_{q_1}(\vec{p}_{q_1})$ derived from the eigenmode $\phi^{(+)}_{q_1, \lambda_1}(\vec{r})$ [36,39–41] as

$$G_{q_1}(\vec{p}_{q_1}) = \frac{i\pi\mathcal{N}_{q_1}}{2\alpha_{q_1}\omega_{q_1}}\left[\frac{\epsilon_{q_1}(\vec{p}_{q_1})}{E_{q_1}(\vec{p}_{q_1})}\right]^{\frac{1}{2}} \times [E_{q_1}(\vec{p}_{q_1}) + E_{q_1}]\exp\left(-\frac{\vec{p}_{q_1}{}^2}{4\alpha_{q_1}}\right). \quad (18)$$

Similar expression for $\tilde{G}_{\bar{q}_2}(\vec{p} - \vec{p}_{q_1})$ is realized from the eigenmode $\phi^{(-)}_{q_2,\lambda_2}(\vec{r})$ [38–41] so as to get, for like flavors,

$$\tilde{G}_{\bar{q}_2}(\vec{p} - \vec{p}_{q_1}) = G^{\star}_{\bar{q}_2}(\vec{p} - \vec{p}_{q_1}). \quad (19)$$

Here, $E_{q_j}(\vec{p}_{q_j}) = \sqrt{\vec{p}^2_{q_j} + m^2_{q_j}}$ and $\epsilon_{q_j}(\vec{p}_{q_j}) = E_{q_j}(\vec{p}_{q_j}) + m_{q_j}$ and $(\mathcal{N}_{q_j}, E_{q_j}, \omega_{q_j}, \alpha_{q_j})$ are the model quantities as defined in Refs. [37–41].

We may point out here that although the three-momentum conservation is ensured explicitly in this model through $\delta^{(3)}(\vec{p}_{q_1} + \vec{p}_{q_2} - \vec{p})$ in the meson state $|M(\vec{p}, S_M)\rangle$, it is not so explicit in the case of energy conservation. This is, of course, true with almost all the potential models that describe the meson as a bound state of valance quark and antiquark interacting via some instantaneous potential. However, we have realized in previous applications of this model [40] in the context of radiative leptonic decays of B, B_c, D and D_s^- mesons that the effective momentum distribution function $\mathcal{G}_M(\vec{p}_{q_1}, \vec{p}_{q_2})$ in Eqs. (17)–(19) somehow ensures energy conservation in an average sense satisfying $E_M = \langle M(\vec{p}, S_M)\,|\,[E_{q_1}(\vec{p}_{q_1}) + E_{q_2}(\vec{p}_{q_2})]\,|\,M(\vec{p}, S_M)\rangle$. The bound state character of the meson represented by the appropriate wave packet (15) is embedded in the dynamical quantity $\mathcal{G}_M(\vec{p}_{q_1}, \vec{p} - \vec{p}_{q_1})$ derivable in this model.

With this phenomenological picture showing dynamics of the constituent particles inside the participating meson bound state, one can obtain the decay amplitudes in terms of model quantities.

Now, considering the factorized amplitudes in Eq. (1) and the appropriate wave packets for participating meson states $|M(\vec{p}, S_M)\rangle$ and $|P_1(\vec{k}, S_{P_1})\rangle$, the S-matrix element for the process $M \to P_1P_2$ can be obtained in the form

$$S_{fi} = -i\frac{G_F}{\sqrt{2}}V_{q_{1(2)}q'_{1(2)}}V_{q_3q'_3}a_1h'^{\mu}H'_{\mu}, \quad (20)$$

where

$$h'^{\mu} = \langle P_2(\vec{q}, S_{P_2})|J^{\mu}|0\rangle, \quad (21)$$

$$H'_{\mu} = \langle P_1(\vec{k}, S_{P_1})|J_{\mu}|M(\vec{p}, S_M)\rangle = \frac{1}{\sqrt{N_M(\vec{p})N_{P_1}(\vec{k})}}\int\frac{d^3\vec{p}_{q_j}\mathcal{G}_M(\vec{p}_{q_j}, \vec{p} - \vec{p}_{q_j})\mathcal{G}_{P_1}(\vec{p}_{q_j} + \vec{k} - \vec{p}, \vec{p} - \vec{p}_{q_j})}{\sqrt{(2\pi)^4 2E_{q_j}(\vec{p}_{q_j})2E_{q'_j}(\vec{p}_{q_j} + \vec{k} - \vec{p})}} \times \delta^{(4)}(p_{q_{1(2)}} - p_{q'_{1(2)}} - p_{q_3} - p'_{q_3})\langle S_{P_1}|J_{\mu}|S_M\rangle. \quad (22)$$

Here, $E_{q_j}(\vec{p}_{q_j})$ and $E_{q'_j}(\vec{p}_{q_j} + \vec{k} - \vec{p})$ stand for the energy of the nonspectator quark or antiquark of the parent and daughter meson, respectively. $\langle S_{P_1}|J_{\mu}|S_M\rangle$ represents symbolically the spin matrix elements of the vector-axial vector current. For the transitions involving nonspectator quark q_1, the spin matrix element is obtained in the form

$$\langle S_{P_1}|J_{\mu}|S_M\rangle = \sum_{\lambda_1,\lambda'_1,\lambda_2}\zeta^{M}_{q_1,q_2}(\lambda_1, \lambda_2)\zeta^{P_1}_{q'_1,q_2}(\lambda'_1, \lambda_2) \times [\bar{U}_{q'_1}(\vec{k} + \vec{p}_{q_1} - \vec{p}, \lambda'_1)\gamma_{\mu} \times (1 - \gamma_5)U_{q_1}(\vec{p}_{q_1}, \lambda_1)], \quad (23)$$

where $\zeta^{M}(\lambda_1, \lambda_2)$ and $\zeta^{P_1}(\lambda'_1, \lambda_2)$ are the appropriate SU(6) spin-flavor coefficients for the parent and daughter meson, respectively. The hadronic amplitude for the transition involving the antiquark $\bar{q}_2$ decay can be obtained in the similar form (23). The relevant spin matrix element is obtained by replacement of free particle spinors as $U_{q_1}(\vec{p}_{q_1}, \lambda_1) \to V_{q'_2}(\vec{k} + \vec{p}_{q_2} - \vec{p}, \lambda'_2)$ and $\bar{U}_{q'_1}(\vec{p}_{q_1} + \vec{k} - \vec{p}, \lambda'_1) \to \bar{V}_{q_2}(\vec{p}_{q_2}, \lambda_2)$. Here, the free particle spinors $U_{q_j}(\vec{p}_{q_j}, \lambda_j)$ and $V_{q_j}(\vec{p}_{q_j}, \lambda_j)$ are taken in the form

$$U_{q_j}(\vec{p}_{q_j}, \lambda_j) = \sqrt{\epsilon_{q_j}(\vec{p}_{q_j})}\begin{pmatrix}\chi(\lambda)\\ \frac{\vec{\sigma}.\vec{p}_{q_j}}{\epsilon_{q_j}(\vec{p}_{q_j})}\chi(\lambda)\end{pmatrix}$$
$$V_{q_j}(\vec{p}_{q_j}, \lambda_j) = \sqrt{\epsilon_{q_j}(\vec{p}_{q_j})}\begin{pmatrix}\tilde{\chi}(\lambda)\\ \frac{\vec{\sigma}.\vec{p}_{q_j}}{\epsilon_{q_j}(\vec{p}_{q_j})}\tilde{\chi}(\lambda)\end{pmatrix}, \quad (24)$$

with

$$\chi(\uparrow) = -\tilde{\chi}(\downarrow) = \begin{pmatrix}1\\0\end{pmatrix}, \qquad \chi(\downarrow) = \tilde{\chi}(\uparrow) = \begin{pmatrix}0\\1\end{pmatrix}.$$

As described above, we assume the energy conservation at the composite level with $E_M = E_{q_1}(\vec{p}_{q_1}) + E_{q_2}(\vec{p} - \vec{p}_{q_1})$. This, together with the explicit three-momentum conservation constraint $\vec{p} = \vec{p}_{q_1} + \vec{p}_{q_2}$ and $\vec{k} = \vec{p}_{q'_{1(2)}} + \vec{p}_{q_{2(1)}}$, enables one to write $p = p_{q_1} + p_{q_2}$ and $k = p_{q'_{1(2)}} + p_{q_{2(1)}}$. Thus, one can pull out $\delta^{(4)}(p_{q_{1(2)}} - p_{q'_{1(2)}} - p_1 - p_2)$ from the quark-level integral of S_{fi} (20) in the form of the meson level four-momentum delta function $\delta^{(4)}(p - k - q)$ to write the S-matrix element in the form

$$S_{fi} = (2\pi)^4\delta^{(4)}(p - q - k)(-i\mathcal{M}_{fi}) \times \frac{1}{\sqrt{V2E_M}}\prod_f\left(\frac{1}{\sqrt{V2E_f}}\right). \quad (25)$$

We may also point out that the normalization factors $\frac{1}{\sqrt{V2E_M}}$, $\frac{1}{\sqrt{V2E_{P_1}}}$ and $\frac{1}{\sqrt{V2E_{P_2}}}$ for the initial and final meson states do not appear automatically in the kinematic expression for S_{fi}. We, therefore, incorporate these factors by adequately compensating the same in the numerator. The compensating factor $\sqrt{2E_M 2E_{P_1}}$ relevant for the matrix element $H'_\mu = \langle P_1(\vec{k}, S_{P_1})|J_\mu|M(\vec{p}, S_M)\rangle$ is then pushed inside the integral (23) as $\sqrt{2[E_{q_1}(\vec{p}_{q_j}) + E_{q_2}(\vec{p} - \vec{p}_{q_j})]2[E_{q'_{1(2)}}(\vec{p}_{q_j} + \vec{k} - \vec{p}) + E_{q_{2(1)}}(\vec{p} - \vec{p}_{q_j})]}$ under the same assumption for energy conservation mentioned earlier. The modified overlapping integral H'_μ is, hereafter, to be written as H_μ. The factor $\sqrt{\frac{2E_{P_2}}{(2\pi)^3}}$, together with $\langle P_2(\vec{q}, S_{P_2})|J^\mu|0\rangle$, defines the covariant matrix element, hereafter to be written as h^μ, which can be parametrized as $if_{P_2}p^\mu_{P_2}$. The meson level S-matrix element is then expressed in the standard form from which the invariant transition amplitude can be obtained in the parent meson rest frame as

$$\mathcal{M}_{fi} = \frac{G_F}{\sqrt{2}} V_{q_{1(2)}q'_{1(2)}} V_{q_3 q'_3} a_1 \mathcal{A}. \tag{26}$$

Here, $\mathcal{A} = h^\mu H_\mu$ with

$$h^\mu = \sqrt{\frac{2E_{P_2}}{(2\pi)^3}} h'^\mu = if_{P_2} p^\mu_{P_2} \tag{27}$$

and

$$H_\mu = \frac{1}{\sqrt{N_M(0)N_{P_1}(\vec{k})}} \int \frac{d^3\vec{p}_{q_j} \mathcal{G}_M(\vec{p}_{q_j}, -\vec{p}_{q_j}) \mathcal{G}_{P_1}(\vec{p}_{q_j} + \vec{k}, -\vec{p}_{q_j})}{\sqrt{E_{q_j}(\vec{p}_{q_j}) E_{q'_j}(\vec{p}_{q_j} + \vec{k})}}$$
$$\times \sqrt{[E_{q_1}(\vec{p}_{q_j}) + E_{q_2}(-\vec{p}_{q_j})][E_{q'_{1(2)}}(\vec{p}_{q_j} + \vec{k}) + E_{q_{2(1)}}(-\vec{p}_{q_j})]} \langle S_{P_1}|J_\mu(0)|S_M\rangle. \tag{28}$$

Applying usual spin algebra and simplifying for the nonvanishing vector current part, it is straightforward to find from (28) the expressions for the timelike and spacelike parts of the hadronic matrix element, respectively, as

$$\langle P_1(\vec{k})|V_0|M(0)\rangle = H_0 = \int d\vec{p}_{q_j} \mathcal{C}(\vec{p}_{q_j}) \{[E_{q_j}(\vec{p}_{q_j}) + m_{q_j}][E_{q'_j}(\vec{p}_{q_j} + \vec{k}) + m_{q'_j}] + \vec{p}^2_{q_j}\} \tag{29}$$

and

$$\langle P_1(\vec{k})|V_i|M(0)\rangle = H_i = \int d\vec{p}_{q_j} \mathcal{C}(\vec{p}_{q_j}) [E_{q_j}(\vec{p}_{q_j}) + m_{q_j}] k_i, \tag{30}$$

where

$$\mathcal{C}(\vec{p}_{q_j}) = \frac{\mathcal{G}_M(\vec{p}_{q_j}, -\vec{p}_{q_j}) \mathcal{G}_{P_1}(\vec{p}_{q_j} + \vec{k}, -\vec{p}_{q_j})}{\sqrt{N_M(0)N_{P_1}(\vec{k})}} \frac{\sqrt{[E_{q_1}(\vec{p}_{q_1}) + E_{q_2}(-\vec{p}_{q_1})][E_{q'_{1(2)}}(\vec{p}_{q_j} + \vec{k}) + E_{q_{2(1)}}(-\vec{p}_{q_j})]}}{\sqrt{E_{q_j}(\vec{p}_{q_j}) E_{q'_j}(\vec{p}_{q_j} + \vec{k})[E_{q_j}(\vec{p}_{q_j}) + m_{q_j}][E_{q'_j}(\vec{p}_{q_j} + \vec{k}) + m_{q'_j}]}}. \tag{31}$$

Now we compare these results (29)–(31) with covariant factorized amplitudes (4)–(6) and obtain the Lorentz invariant form factors $f_\pm(q^2)$ in the form

$$f_\pm(q^2) = \frac{1}{2} \int d\vec{p}_{q_j} \mathcal{C}(\vec{p}_{q_j}) \{[E_{q_j}(\vec{p}_{q_j}) + m_{q_j}][E_{q'_j}(\vec{p}_{q_j} + \vec{k}) + m_{q'_j}] + \vec{p}^2_{q_j} \pm [E_{q_j}(\vec{p}_{q_j}) + m_{q_j}][M \mp E_{P_1}]\}. \tag{32}$$

Then the model expression for the form factor $F_0(q^2)$ is obtained from $F_0(q^2) = [\frac{q^2}{(M^2 - m_1^2)}] f_-(q^2) + f_+(q^2)$ in terms of which the decay width $\Gamma(M \to P_1 P_2)$ is expressed as

$$\Gamma(M \to P_1 P_2) = \frac{|\vec{k}|}{8\pi M^2} |\mathcal{A}_1|^2 |F_0(q^2)|^2, \tag{33}$$

where

$$|\mathcal{A}_1| = \frac{G_F}{\sqrt{2}} V_{q_{1(2)}q'_{1(2)}} V_{q_3 q'_3} a_1 (M^2 - m^2_{P_1}) f_{P_2}. \tag{34}$$

B. $M \to PV$

The two-body nonleptonic decay process in this category is also characterized by external W-boson emission which hadronizes to a vector meson (V) instead of a pseudoscalar meson. The other final state meson is a

pseudoscalar (P) which is coupled to the decaying meson (M), providing hadronic amplitude of the decay process. It is trivial to check that the decay amplitude in the parent meson rest frame is expressed here in terms of $F_1(q^2)$ instead of $F_0(q^2)$ as

$$\langle P(\vec{k})V(\vec{q})|\mathcal{H}_{\rm eff}|M(0)\rangle = i\frac{G_F}{\sqrt{2}}V_{q_{1(2)}q'_{1(2)}}V_{q_3q'_3}2a_1 m_V f_V F_1(q^2)(e^\star\cdot p). \quad (35)$$

Using a similar technique as used in calculating the transition $M\to P_1P_2$, the form factor $F_1(q^2)$ in the parent meson rest frame is obtained in the form

$$\begin{aligned}F_1(q^2) &= f_+(q^2)\\ &= \frac{1}{2}\int d\vec{p}_{q_j}\mathcal{C}(\vec{p}_{q_j})\{[E_{q_j}(\vec{p}_{q_j})+m_{q_j}]\\ &\quad\times[E_{q'_j}(\vec{p}_{q_j}+\vec{k})+m_{q'_j}]+\vec{p}^{\,2}_{q_j}\\ &\quad+[E_{q_j}(\vec{p}_{q_j})+m_{q_j}][M-E_P]\},\end{aligned} \quad (36)$$

in terms of which the decay width $\Gamma(M\to PV)$ is expressed as

$$\Gamma(M\to PV) = \frac{|\vec{k}|^3}{8\pi m_V^2}|\mathcal{A}_2|^2|F_1(q^2)|^2, \quad (37)$$

where

$$|\mathcal{A}_2| = \frac{G_F}{\sqrt{2}}V_{q_{1(2)}q'_{1(2)}}V_{q_3q'_3}2a_1 m_V f_V. \quad (38)$$

C. $M\to VP$

In the decay process of this category, the externally emitted W boson hadronizes to a pseudoscalar meson (P) and other final state meson is a vector meson (V) which couples to the decaying meson (M) to give hadronic amplitude of the decay process. It is trivial to see that the vector part of weak current does not contribute and the nonvanishing decay amplitude, due to the axial vector part in the parent meson rest frame, is obtained in the simple form

$$\langle V(\vec{k})P(\vec{q})|\mathcal{H}_{\rm eff}|M(0)\rangle = i\frac{G_F}{\sqrt{2}}V_{q_{1(2)}q'_{1(2)}}V_{q_3q'_3}2a_1 m_V f_P A_0(q^2)(e^\star\cdot p). \quad (39)$$

Although the decay amplitude in this case is expected to depend upon four form factors (A_1, A_2, A_3 and A_0), it is in fact reduced to the simple form (39) involving only a single form factor $A_0(q^2)$. This is due to the mutual cancellation of the terms due to the linear relation (9). With the appropriate wave packet description for the participating meson states $|V(\vec{k},S_V)\rangle$ and $|M(\vec{p},S_V)\rangle$, it is straightforward to calculate the nonvanishing factorized amplitude $\langle V(\vec{k},S_V)|A_\mu|M(0,S_M)\rangle$ so as to arrive at the invariant decay amplitude similar to (26)–(28). However, the spin matrix elements $\langle S_V|A_\mu|S_M\rangle$ in these processes are calculated separately for three specific spin states ($S_V=\pm1,0$) of the vector meson (V) which are subsequently generalized to give the model expressions for the timelike and spacelike parts, respectively, in the parent meson rest frame as

$$\langle V(\vec{k},S_V)|A_0|M(0,S_M)\rangle = \int d\vec{p}_{q_j}\mathcal{C}(\vec{p}_{q_j})[E_{q_j}(\vec{p}_{q_j})+m_{q_j}](\hat{e}^\star\cdot\vec{k}) \quad (40)$$

and

$$\begin{aligned}\langle V(\vec{k},S_V)|A_i|M(0,S_M)\rangle &= \int d\vec{p}_{q_j}\mathcal{C}(\vec{p}_{q_j})\{[E_{q_j}(\vec{p}_{q_j})+m_{q_j}]\\ &\quad\times[E_{q'_j}(\vec{p}_{q_j}+\vec{k})+m_{q'_j}]-\vec{p}^{\,2}_{q_j}/3\}\hat{e}^\star.\end{aligned} \quad (41)$$

We then compare expressions in (40) and (41) with corresponding expressions of the covariant factorized amplitudes (7) and (8) and then simplify to obtain the model expression of the form factor $A_0(q^2)$ as

$$\begin{aligned}A_0(q^2) &= \frac{1}{2}\int d\vec{p}_{q_j}\mathcal{C}(\vec{p}_{q_j})\{[E_{q_j}(\vec{p}_{q_j})\\ &\quad+m_{q_j}][M-E_V][E_{q_j}(\vec{p}_{q_j})\\ &\quad+m_{q_j}][E_{q'_j}(\vec{p}_{q_j}+\vec{k})+m_{q'_j}]-\vec{p}^{\,2}_{q_j}/3\}.\end{aligned} \quad (42)$$

The decay width $\Gamma(M\to VP)$ is then obtained in terms of $A_0(q^2)$ in the straightforward manner as

$$\Gamma(M\to VP) = \frac{|\vec{k}|^3}{8\pi m_V^2}|\mathcal{A}_3|^2|A_0(q^2)|^2, \quad (43)$$

where

$$|\mathcal{A}_3| = \frac{G_F}{\sqrt{2}}V_{q_{1(2)}q'_{1(2)}}V_{q_3q'_3}2a_1 m_V f_P. \quad (44)$$

The two-body nonleptonic decays described above refer to class I decays involving external emission of the W boson [Fig. 1(a)]. One can similarly analyze the class II decays that involve internal emission of the W boson [Fig. 1(b)] and also class III decays characterized by both external and internal emission of the W boson [Fig. 1(c)], yielding to P_1P_2, PV and VP final meson states. The model expressions for form factors and decay widths for the later two classes of decays can be obtained by suitable replacement of flavor degrees of freedom, constituent quark masses, quark binding energies, QCD factors a_i and the decay constants in the relevant expressions described above.

IV. NUMERICAL RESULTS AND DISCUSSION

For numerical calculation, we take the flavor-independent potential parameters (a, V_0) and other model

quantities such as the constituent quark masses m_q and corresponding binding energies E_q [38–41] as

$$\begin{aligned}(m_u &= m_d, m_s, m_c, m_b)\\ &\equiv (0.07875, 0.31575, 1.49276, 4.77659)\ \text{GeV}\\ (E_u &= E_d, E_s, E_c, E_b)\\ &\equiv (0.47125, 0.59100, 1.57951, 4.76633)\ \text{GeV}\\ (a, V_0) &\equiv (0.017166\ \text{GeV}^3, -0.1375\ \text{GeV}).\end{aligned} \tag{45}$$

The B_c-meson mass and lifetime, as well as CKM parameters used here, are taken from Ref. [50] as

$$\begin{aligned}(M, \tau_{B_c}) &\equiv (6.277\ \text{GeV}, 0.453\ \text{ps})\\ (|V_{cb}|, |V_{ub}|) &\equiv (0.0409, 0.00415)\\ (|V_{cd}|, |V_{cs}|) &\equiv (0.23, 1.006)\\ (|V_{ud}|, |V_{us}|) &\equiv (0.97425, 0.2252).\end{aligned} \tag{46}$$

The relevant decay constants used in our calculation are taken from Refs. [50,51] as

$$\begin{aligned}&(f_\pi, f_K, f_D, f_{D_s}, f_\eta)\\ &\quad\equiv (0.13041, 0.1561, 0.2067, 0.26, 0.4)\ \text{GeV}\\ &(f_\rho, f_{K^\star}, f_{D^\star}, f_{D_s^\star}, f_{J/\psi})\\ &\quad\equiv (0.221, 0.22, 0.245, 0.273, 0.411)\ \text{GeV}.\end{aligned} \tag{47}$$

For evaluating decay amplitudes of color-suppressed class-II B_c decays involving neutral meson $\pi^0(\rho^0)$ in the final state, we take the corresponding values of the decay constant as $f_{\pi^0(\rho^0)} = f_{\pi^-(\rho^-)}/\sqrt{2}$.

It may be mentioned that the theoretical predictions on nonleptonic decays suffer from uncertainties due to a number of factors such as the model parameters, CKM parameters, decay constants, QCD coefficients a_i, etc. At the outset we would like to point out that our intention here is not to claim a quantitative precision in our prediction but to provide an order of magnitude estimation in order to test the applicability of our model in this sector. For this we use in our numerical calculation the potential parameters and other model quantities, like the quark masses and corresponding binding energies [Eq. (45)], that have already been fixed once at the static level application of our model [37], providing adequate description of wide-ranging hadronic phenomena in the light- and heavy-flavor sector [38–41]. As such, we do not have any free parameter that could be fine tuned from time to time in predicting different hadronic properties as stated above. With these inputs, we perform, in a sense, a parameter-free calculation to test applicability of the model in this sector. In order to minimize uncertainties in our calculation due to the CKM parameter and decay constant, we take the central values of the respective observed data from Ref. [50]. In those cases where experimental data are not available, we take the predicted decay constants [51] used in other quark-model calculations.

As regards QCD coefficients, different values of a_1 and significantly different values of a_2 have been used in the literature. For example in Ref. [14], authors use QCD coefficients Set 1: $(a_1^b, a_2^b) = (1.12, -0.26)$ and $(a_1^c, a_2^c) = (1.26, -0.51)$ as fixed in Ref. [52], whereas most of the previous calculations referred to in Tables V and VI use a different set of QCD coefficients, Set 2: $(a_1^b, a_2^b) = (1.14, -0.2)$ and $(a_1^c, a_2^c) = (1.2, -0.317)$ fixed by Buras *et al.* in the mid 1980s. In order to gauge uncertainty in our prediction due to QCD coefficients, we use both sets in our calculation.

We would also like to point out that the energy conservation ansatz taken here in the parent meson rest frame, $E_{q_1}(\vec{p}_{q_1}) + E_{q_2}(-\vec{p}_{q_1}) = M$, might lead to spurious kinematic singularities at the quark-level integration. We address this issue as in Ref. [13,40] by assigning a running mass, $m_{q_1}(\vec{p}_{q_1})$, to the active quark q_1 in the meson state $|M(0)\rangle$ in the form

$$m_{q_1}^2(\vec{p}_{q_1}) = M^2 - m_{q_2}^2 - 2M\sqrt{|\vec{p}_{q_1}|^2 + m_{q_2}^2}, \tag{48}$$

as an outcome of the energy conservation constraint, while retaining definite mass m_{q_2} of the spectator quark q_2. This leads to an upper bound on the quark momentum $|\vec{p}_{q_1}| < \frac{M^2 - m_{q_2}^2}{2M} = |\vec{p}_{q_1}|_{\max}$ in order to retain $m_{q_1}^2(|\vec{p}_{q_1}|)$ positive definite. The shape of the radial momentum distribution amplitude $|\vec{p}_{q_j}|\mathcal{G}_M(\vec{p}_{p_{q_j}}, -\vec{p}_{q_j})$ over the allowed range $0 < |\vec{p}_{q_j}| < |\vec{p}_{q_j}|_{\max}$ in the present model in the context of radiative leptonic decays of B_u, B_c, D and D_s mesons [41] is obtained in good agreement with that of the QCD relativistic quark model [13]. The rms value of quark momentum $\sqrt{\langle \vec{p}_{q_j}^2 \rangle}$ with $\langle \vec{p}_{q_j}^2 \rangle = \langle M(0)|\vec{p}_{q_j}{}^2|M(0)\rangle$, the expectation values of the quark and antiquark binding energies $\langle E_{q_1}(\vec{p}_{q_1}^2)\rangle$ and $\langle E_{q_2}(-\vec{p}_{q_1}^2)\rangle$, and that of the sum of binding energies $\langle [E_{q_1}(|\vec{p}_{q_1}|^2) + E_{q_2}(|-\vec{p}_{q_1}|^2)]\rangle$ in this model [41] are shown in Table I.

The results show that the rms value of the quark momentum in the meson bound state is much less than the corresponding upper bound $|\vec{p}_{q_j}|_{\max}$, as expected. The average energies of the constituent quark of the same flavor in different meson bound states do not exactly match (Table I). This is due to different kinematics involved from one meson state to the other. The constituent quarks in the meson bound state are considered to be free particles of definite momenta, each associated with the momentum probability amplitude derivable in this model from respective energy eigenmodes via momentum projection. On the other hand, the energies shown in Eq. (45) are the energy eigenvalues of the corresponding bound quarks with no definite momenta of their own and are obtained in this model from respective quark orbitals by solving the Dirac

TABLE I. The rms value of the quark momenta, expectation values of the quark and antiquark energies and that of the combined quark-antiquark energies in the meson state.

Meson state $\|M(0)\rangle$	$\sqrt{\langle \vec{p}_{q_j}^2 \rangle}$ (GeV)	$\langle E_{q_1}(\vec{p}_{q_1}^2) \rangle$ (GeV)	$\langle E_{q_2}(\|-\vec{p}_{q_1}\|^2) \rangle$ (GeV)	$\langle [E_{q_1}(\vec{p}_{q_1}^2) + E_{q_2}(\|-\vec{p}_{q_1}\|^2)] \rangle$ (GeV)	Observed meson mass (GeV) [50]
$\|B_u(0)\rangle$	0.51	4.799	0.480	5.279	5.27925
$\|B_c(0)\rangle$	0.66	4.657	1.629	6.286	6.277
$\|D_s(0)\rangle$	0.4736	1.4165	0.5517	1.9682	1.96849
$\|D(0)\rangle$	0.4506	1.4418	0.4275	1.8693	1.86962

equation. These energy eigenvalues in Eq. (45) should be different from the average energy of the constituent quarks (Table I). The marginal difference, in energies, shown in Table I and Eq. (45) does not affect the result as is evident from our predicted meson masses in good agreement with their respective observed values [Table I]. This lends credence to our energy conservation ansatz in an average sense through effective momentum distribution function $\mathcal{G}_M(\vec{p}_{q_1}, -\vec{p}_{q_1})$ in the meson state $|M(0)\rangle$.

Now using input parameters (45)–(47), we first evaluate the weak form factors $F_0(q^2)$, $F_1(q^2)$ and $A_0(q^2)$ from Eqs. (32), (36), and (42), respectively, and study their q^2 dependence in the allowed kinematical range. In a self-consistent dynamical approach, we extract the weak form factors from overlap integrals of meson wave functions where q^2 dependence is automatically ensured in the entire kinemtical range. This is in contrast to most of the previous model approaches, where the form factors were determined only at one kinematical point, either at $q^2 \to 0$ or $q^2 \to q^2_{\rm max}$, and then extrapolated to allowed kinematical range using some phenomenological ansatz (mainly di (pole) or Gaussian). Figures 2–6 depict the q^2 dependence of the form factors for different decay modes. We find large overlapping of meson wave functions in this model as shown in Figs. 7 and 8. Our predicted form factors at maximum recoil point ($q^2 \to 0$): $F_0(0)^{M\to m_1} = F_1(0)^{M\to m_1}$ for $B_c \to P$ transitions satisfies the requirement for pole cancellation at that point. Our predictions for form factors at $q^2 \to 0$ in $b \to u$, c and $\bar{c} \to \bar{s}$, $\bar{d}$-induced decays shown in Table II are found greater than those of Ref. [14] by a factor of about 2 except for the form factor relating $B_c \to V$ in $b \to c$, u-induced decays only which is found about 2.5 times smaller.

We then evaluate decay widths $\Gamma(B_c \to m_1 m_2)$ from Eqs. (33), (37), and (43) and our results are listed in Tables III and IV for general values of QCD coefficients $a_{1,2}$ to facilitate a comparison with other model predictions. Our predictions for various tree-level, two-body nonleptonic B_c-meson decays with respect to both sets of

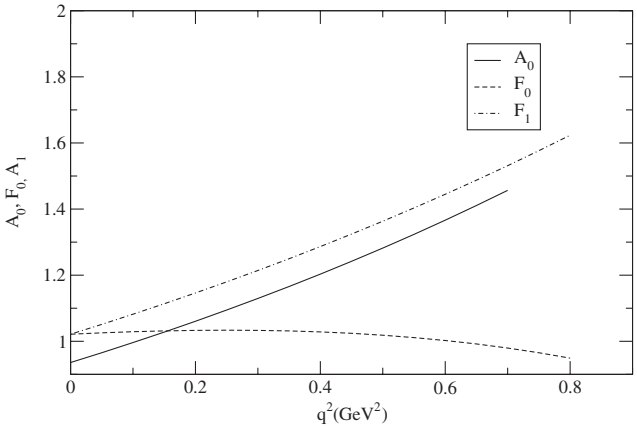

FIG. 3. Form factors of $B_c \to B_s$, $B_s^\star$.

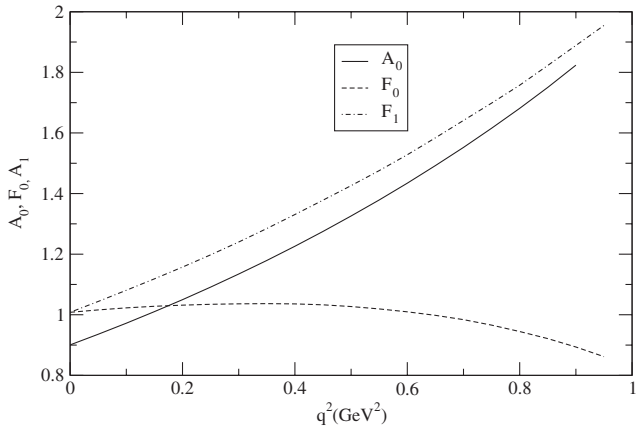

FIG. 2. Form factors of $B_c \to B$, $B^\star$.

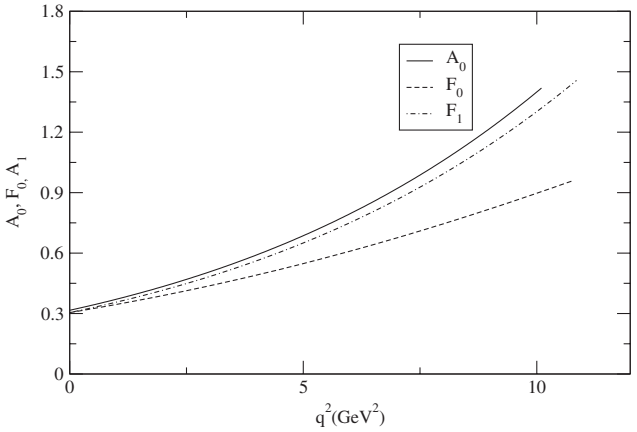

FIG. 4. Form factors of $B_c \to \eta_c$, J/Ψ.

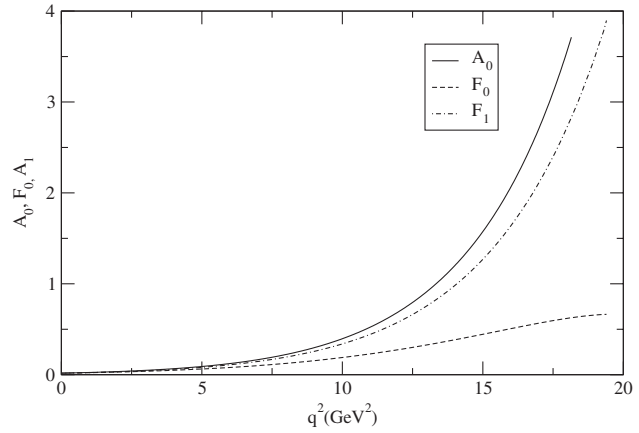

FIG. 5. Form factors of $B_c \to D, D^*$.

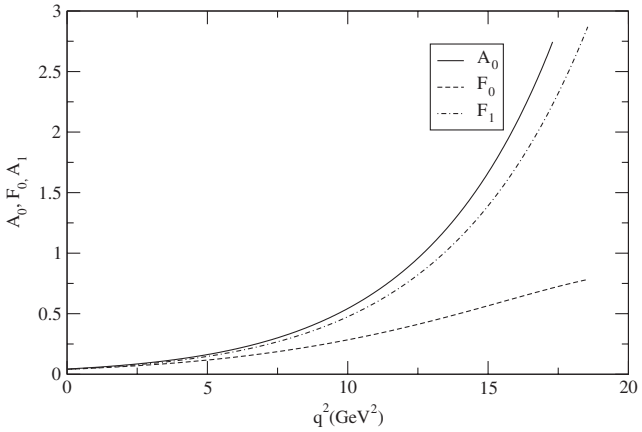

FIG. 6. Form factors of $B_c \to D_s, D_s^\star$.

QCD coefficients are shown in the second column of Tables V and VI: one corresponds to Set 1 and other, in the parentheses, corresponds to Set 2. The predicted branching ratios with Set 1 QCD coefficients, though, do not exactly match with those in Set 2; however, the order of magnitude in both cases remains same in the range $\mathcal{O}(10^{-6}$–$10^{-2})$ in broad agreement with other quark model predictions.

For $\bar{c} \to \bar{s}$, $\bar{d}$-induced decays, our predicted branching ratios in most of the cases find an order of magnitude agreement with the predictions of Refs. [7,8] and in a few cases such as $B_c^- \to \bar{B}_s^0 K^-$, $B^-(K^{0\star}, K^0)$ with those of Refs. [11,12]. The most promising decay modes found in this category are $B_c^- \to \bar{B}_s^0 \pi^-$, $\bar{B}_s^0 \rho^-$, $\bar{B}_s^{0\star} \pi^-$ with large predicted branching ratios of 12.01, 9.96 and 8.61%, respectively, which should be experimentally accessible.

Summing up exclusive contributions, these decay modes are found to contribute about 42% of the total branching ratio compared to 70% as estimated in Ref. [4]. Our predicted summed-up exclusive branching ratio, although found smaller than 73.4% as predicted in the QCD sum rule [7], is however comparable to the relativistic constituent

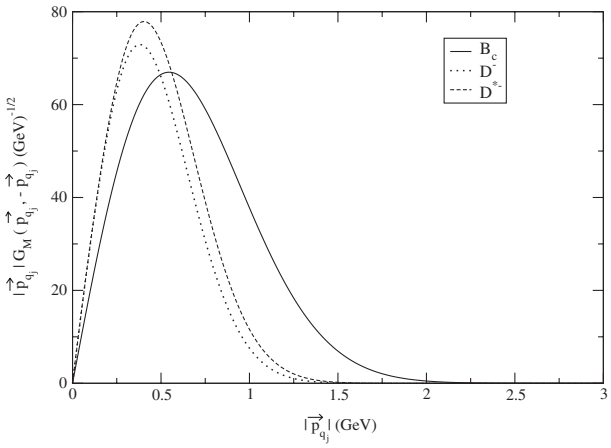

FIG. 7. Radial quark momentum distribution amplitude $|\vec{p}_{q_1}|\mathcal{G}_M(\vec{p}_{q_1}, -\vec{p}_{q_1})$ versus $|\vec{p}_{q_1}|$ for B_c, D^- and D^{-*} meson.

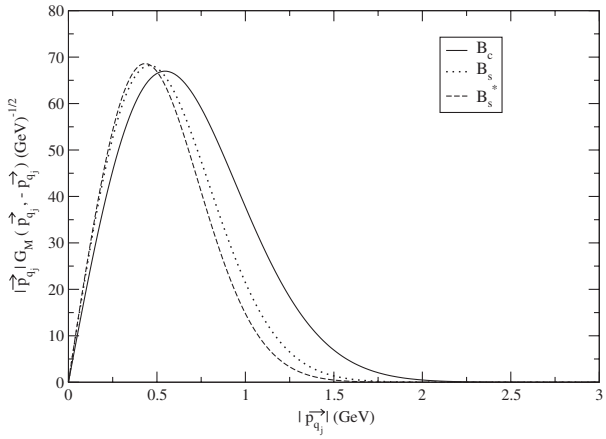

FIG. 8. Radial quark momentum distribution amplitude $|\vec{p}_{q_1}|\mathcal{G}_M(\vec{p}_{q_1}, -\vec{p}_{q_1})$ versus $|\vec{p}_{q_1}|$ for B_c, B_s and B_s^* meson.

quark model [9] prediction of 27.6%. The B_c meson, therefore, can be the source of the B_s meson, as copious production of the B_c meson is expected at LHC.

For $b \to c$, u-induced decays, our results are in general agreement with the QCD sum rule [7] and constitute quark-model [8,10–12] predictions. The dominant modes found in this category are $B_c^- \to \eta_c(D_s^-, D_s^{-\star})$, $\eta_c \rho^-$ and $J/\Psi D_s^-$ with predicted branching ratios of 0.18, 0.15, 0.106 and 0.115%, respectively, which should also be

TABLE II. Form factors of $B_c \to P$, V transitions at $q^2 = 0$.

Quark level decay	Transitions	$F_0^{B_c \to P}(0)$	$F_1^{B_c \to P}(0)$	$A_0^{B_c \to V}(0)$
$\bar{c} \to \bar{s}, \bar{d}$	$B_c \to B, B^*$	1.01	1.01	0.90
	$B_c \to B_s, B_s^*$	1.03	1.03	0.94
$b \to c, u$	$B_c \to \eta_c, J/\Psi$	0.30	0.30	0.325
	$B \to D, D^*$	0.025	0.025	0.025
	$B \to D_s, D_s^*$	0.05	0.05	0.05

TABLE III. Exclusive nonleptonic decay widths for the B_c decays in units of 10^{-15} GeV for general values of the effective Wilson coefficients a_1 and a_2.

Quark level decay	Decay	Modes	Decay width
	$B_c^- \to PP$	$B_c^- \to \eta_c \pi^-$	$0.391a_1^2$
		$B_c^- \to \eta_c K^-$	$0.031a_1^2$
		$B_c^- \to \eta_c D_s^-$	$(1.82a_1 + 1.6a_2)^2$
		$B_c^- \to \eta_c D^-$	$(0.32a_1 + 0.24a_2)^2$
	$B_c^- \to PV$	$B_c^- \to \eta_c \rho^-$	$1.23a_1^2$
$b \to c, u$		$B_c^- \to \eta_c K^{*-}$	$0.067a_1^2$
		$B_c^- \to \eta_c D_s^{*-}$	$(1.72a_1 + 1.75a_2)^2$
		$B_c^- \to \eta_c D^{*-}$	$(0.35a_1 + 0.29a_2)^2$
	$B_c^- \to VP$	$B_c^- \to J/\Psi \pi^-$	$0.392a_1^2$
		$B_c^- \to J/\Psi K^-$	$0.031a_1^2$
		$B_c^- \to J/\Psi D_s^-$	$(1.6a_1 + 1.87a_2)^2$
		$B_c^- \to J/\Psi D^-$	$(0.28a_1 + 0.30a_2)^2$
	$B_c^- \to PP$	$B_c^- \to \bar{B}_s^0 \pi^-$	$109.94a_1^2$
		$B_c^- \to \bar{B}_s^0 K^-$	$7.30a_1^2$
		$B_c^- \to \bar{B}^0 \pi^-$	$7.23a_1^2$
		$B_c^- \to \bar{B}^0 K^-$	$0.51a_1^2$
		$B_c^- \to B^- K^0$	$181.63a_2^2$
		$B_c^- \to B^- \pi^0$	$3.598a_2^2$
	$B_c^- \to PV$	$B_c^- \to \bar{B}_s^0 \rho^-$	$91.28a_1^2$
		$B_c^- \to \bar{B}_s^0 K^{*-}$	$0.341a_1^2$
		$B_c^- \to \bar{B}^0 \rho^-$	$11.87a_1^2$
$\bar{c} \to \bar{s}, \bar{d}$		$B_c^- \to \bar{B}^0 K^{*-}$	$0.3a_1^2$
		$B_c^- \to B^- K^{*0}$	$102.5a_2^2$
		$B_c^- \to B^- \rho^0$	$5.94a_2^2$
	$B_c^- \to VP$	$B_c^- \to \bar{B}_s^{*0} \pi^-$	$78.82a_1^2$
		$B_c^- \to \bar{B}_s^{*0} K^-$	$4.57a_1^2$
		$B_c^- \to \bar{B}^{*0} \pi^-$	$5.08a_1^2$
		$B_c^- \to \bar{B}^{*0} K^-$	$0.35a_1^2$
		$B_c^- \to B^{*-} K^0$	$126.22a_2^2$
		$B_c^- \to B^{*-} \pi^0$	$2.53a_2^2$

TABLE IV. Exclusive nonleptonic decay widths for the B_c decays into DD mesons in units of 10^{-15} GeV for general values of the effective Wilson coefficients a_1 and a_2.

Quark level decay	Decay	Modes	Decay width
	$B_c^- \to PP$	$B_c^- \to D^- D^0$	$0.027a_2^2$
		$B_c^- \to D_s^- D^0$	$0.006a_2^2$
		$B_c^- \to D^- \bar{D}^0$	$(0.004a_1 + 0.004a_2)^2$
		$B_c^- \to D_s^- \bar{D}^0$	$(0.024a_1 + 0.034a_2)^2$
	$B_c^- \to PV$	$B_c^- \to D^- D^{*0}$	$0.056a_2^2$
$b \to c, u$		$B_c^- \to D_s^- D^{*0}$	$0.011a_2^2$
		$B_c^- \to D^- \bar{D}^{*0}$	$(0.004a_1 + 0.006a_2)^2$
		$B_c^- \to D_s^- \bar{D}^{*0}$	$(0.027a_1 + 0.046a_2)^2$
	$B_c^- \to VP$	$B_c^- \to D^{*-} D^0$	$0.034a_2^2$
		$B_c^- \to D_s^{*-} D^0$	$0.007a_2^2$
		$B_c^- \to D^{*-} \bar{D}^0$	$(0.006a_1 + 0.004a_2)^2$
		$B_c^- \to D_s^{*-} \bar{D}^0$	$(0.031a_1 + 0.037a_2)^2$

accessible experimentally at high-luminosity hadron colliders. The contributions of two charmed meson final states are found too small $\mathcal{O}(10^{-6})$ [Table VII] to be measured experimentally. We would like to mention here that the $b \to u$-induced decays such as $B_c^- \to \bar{D}^0(K^-, \pi^-)$, $D^- \pi^0$ and $D_s^- \pi^0$, where the W boson hadronizes to u, d, s quark/antiquark, are seriously CKM suppressed. Extending our analysis to these decays, we find the branching ratios of $B_c^- \to \bar{D}^0 K^-$, $\bar{D}^0 \pi^-$, $D^- \pi^0$ and $D_s^- \pi^0$ are found to be 1.45×10^{-9}, 1.9×10^{-8}, 5.9×10^{-10} and 1.8×10^{-10}, respectively, which are too small to be experimentally accessible even at the high-luminosity hadron collider. Summing up exclusive contributions, the bottom-changing decay modes considered here are found to contribute barely 0.67% of the total branching ratios against the estimated value of 20% [4], which leaves plenty of room for B_c decays to two vector meson states, excited meson states and nonresonant multibody final states.

The relative size of branching ratios for nonleptonic decays is broadly estimated from power counting of QCD factors and CKM factors in the Wolfenstein parametrization [53]. Accordingly, the class-I decay modes determined by QCD factor a_1 are found to have comparatively large branching ratios, the most promising of which are the CKM-favored ones $B_c^- \to \bar{B}_s^0(\pi^-, \rho^-)$, $\bar{B}_s^{0\star}\pi^-$ as shown in Table VI. On the other hand, the branching ratios of class-II decay modes determined by a_2 are found relatively smaller, as expected, than those of class-I modes. However $B_c^- \to B^-(K^0, K^{0\star})$ decay modes in this category with CKM factor $V_{cs}V_{ud}^* \sim 1$ have been estimated to have branching ratios of 3.36% and 2.34%, respectively which should be measured experimentally.

In class-III decays characterized by the Pauli interference, the branching ratios are determined by relative values of a_1 with respect to a_2. Considering the negative value of a_2 in Set 1 with respect to a_1, these decay modes are found suppressed in comparison with the cases in which interference is switched off. It is also known that, on a qualitative level, the ratio $\frac{a_2}{a_1}$ is a function of running coupling constant α_s evaluated at the factorization scale. This has been shown to be positive for B decays and negative for D decays corresponding to small and large coupling, respectively, [47]. The experimental data also favor constructive interference of color-favored and color-suppressed B-decay modes. Taking into account the positive value of QCD factor $a_2^b = 0.26$ in Set 1, our predicted branching ratios for class-III B_c decays find an enhancement by a factor of about 2 over what was obtained with negative value of $a_2^b = -0.26$ in the same order of magnitude $\sim\mathcal{O}(10^{-6})$. Furthermore, in order to test the effect of interference in these decays, we put the decay width in the form $\Gamma = \Gamma_0 + \Delta\Gamma$, where $\Gamma_0 = x_1 a_1^2 + x_2 a_2^2$ and $\Delta\Gamma = 2x_1 x_2 a_1 a_2$ and compute $\frac{\Delta\Gamma}{\Gamma_0}$ in % as done in Refs. [6,46]. The absolute value of $\frac{\Delta\Gamma}{\Gamma_0}$ for $B_c^- \to D_s^- \bar{D}^0$, $D_s^- \bar{D}^{0\star}$, $D_s^{-\star} \bar{D}^0$, $\eta_c D_s^{-\star}$ and $\eta_c D^{*-}$ are found 59, 68, 51,

TABLE V. Predicted branching ratios (in %) of exclusive nonleptonic B_c decays with the choice of Wilson coefficients Set 1 (Set 2) for b decay in comparison with other model predictions.

Decay mode	This work	Reference [7]	Reference [8]	Reference [12]	Reference [13]	Reference [10]	Reference [11]	Reference [9]	Reference [14]
$B_c^- \to \eta_c \pi^-$	0.034 (0.035)	0.20	0.18	0.13	0.025	0.083	0.14	0.19	0.14
$B_c^- \to \eta_c K^-$	0.003 (0.003)	0.013	0.014	0.013	0.002	0.006	0.011	0.015	...
$B_c^- \to \eta_c D_s^-$	0.179 (0.21)	0.28	0.054	0.35	0.50	...	0.26	0.44	0.52
$B_c^- \to \eta_c D^-$	0.006 (0,007)	0.015	0.0012	0.010	0.005	...	0.014	0.019	...
$B_c^- \to \eta_c \rho^-$	0.106 (0.11)	0.42	0.49	0.30	0.067	0.20	0.33	0.45	0.39
$B_c^- \to \eta_c K^{\star -}$	0.006 (0.006)	0.020	0.025	0.021	0.004	0.011	0.018	0.025	...
$B_c^- \to \eta_c D_s^{\star -}$	0.149 (0.178)	0.27	0.044	0.36	0.057	...	0.24	0.37	0.31
$B_c^- \to \eta_c D^{\star -}$	0.007 (0.008)	0.010	0.0010	0.0055	0.003	...	0.013	0.019	...
$B_c^- \to J/\psi \pi^-$	0.034 (0.035)	0.13	0.18	0.073	0.13	0.060	0.11	0.17	0.13
$B_c^- \to J/\psi K^-$	0.003 (0.003)	0.011	0.014	0.007	0.007	0.005	0.008	0.013	...
$B_c^- \to J/\psi D_s^-$	0.115 (0.142)	0.17	0.041	0.12	0.35	...	0.15	0.34	0.28
$B_c^- \to J/\psi D^-$	0.004 (0.005)	0.009	0.0009	0.0044	0.013	...	0.009	0.015	...

TABLE VI. Predicted branching ratios (in %) of exclusive nonleptonic B_c decays with the choice of Wilson coefficients Set 1 (Set 2) for $\bar{c}$ decay in comparison with other model predictions.

Decay mode	This work	Reference [7]	Reference [8]	Reference [12]	Reference [13]	Reference [10]	Reference [11]	Reference [9]	Reference [14]
$B_c^- \to \bar{B}_s^0 \pi^-$	12.01 (10.9)	16.4	5.75	3.42	3.01	2.46	1.56	3.9	4.8
$B_c^- \to \bar{B}_s^0 K^-$	0.798 (0.723)	1.06	0.41	...	0.21	0.21	0.17	0.29	...
$B_c^- \to \bar{B}^0 \pi^-$	0.79 (0.72)	1.06	0.32	0.15	0.19	0.10	0.10	0.20	...
$B_c^- \to \bar{B}^0 K^-$	0.055 (0.054)	0.07	0.025	...	0.014	0.009	0.010	0.015	...
$B_c^- \to B^- K^0$	3.25 (1.256)	1.98	0.66	0.17	...	0.23	0.27	0.38	0.8
$B_c^- \to B^- \pi^0$	0.064 (0.025)	0.037	0.011	0.007	...	0.003	0.004	0.007	...
$B_c^- \to \bar{B}_s^0 \rho^-$	9.97 (9.05)	7.2	4.41	2.33	1.34	1.38	3.86	2.3	7.0
$B_c^- \to \bar{B}_s^0 K^{\star -}$	0.04 (0.034)	...	...	...	0.0043	0.0030	0.10	0.011	...
$B_c^- \to \bar{B}^0 \rho^-$	1.297 (1.177)	0.96	0.59	0.19	0.15	0.13	0.28	0.20	...
$B_c^- \to \bar{B}^0 K^{\star -}$	0.032 (0.029)	0.015	0.018	...	0.003	0.004	0.012	0.0048	...
$B_c^- \to B^- K^{\star 0}$	1.83 (0.71)	0.43	0.47	0.095	...	0.09	0.32	0.11	0.72
$B_c^- \to B^- \rho^0$	0.106 (0.041)	0.034	0.020	0.009	...	0.005	0.010	0.0071	...
$B_c^- \to \bar{B}_s^{\star 0} \pi^-$	8.61 (7.81)	6.5	5.08	1.95	3.50	1.58	1.23	2.1	4.37
$B_c^- \to \bar{B}_s^{\star 0} K^-$	0.499 (0.453)	0.37	0.29	...	0.16	0.11	0.13	0.13	...
$B_c^- \to \bar{B}^{\star 0} \pi^-$	0.555 (0.503)	0.95	0.29	0.077	0.24	0.026	0.076	0.057	...
$B_c^- \to \bar{B}^{\star 0} K^-$	0.039 (0.035)	0.055	0.019	...	0.012	0.004	0.006	0.0036	...
$B_c^- \to B^{\star -} K^0$	2.26 (0.873)	1.60	0.50	0.061	...	0.10	0.16	0.088	...
$B_c^- \to B^{\star -} \pi^0$	0.047 (0.018)	0.033	0.010	0.004	...	0.001	0.003	0.002	...

TABLE VII. Predicted branching ratios in units of 10^{-6} of the exclusive nonleptonic B_c decays into DD mesons in comparison with other model predictions.

Decay mode	This work	Reference [13]	Reference [11]	Reference [7]	Reference [8]	Reference [15]	Reference [9]	Reference [16]
$B_c^- \to D^- D^0$	1.284 (0.76)	4.1	17	53	18	86	33	32
$B_c^- \to D_s^- D^0$	0.27 (0.16)	0.27	1.13	4.8	0.93	4.6	2.1	2.3
$B_c^- \to D^- \bar{D}^0$	0.008 (0.01)	...	...	0.32	...	...	0.31	0.1
$B_c^- \to D_s^- \bar{D}^0$	0.219 (0.286)	...	...	6.6	...	...	7.4	3.0
$B_c^- \to D^- D^{\star 0}$	2.61 (1.54)	3.6	21	75	19	75	38	34
$B_c^- \to D_s^- D^{\star 0}$	0.491 (0.291)	0.25	1.35	7.1	0.97	3.9	2.4	2.6
$B_c^- \to D^- \bar{D}^{\star 0}$	0.008 (0.011)	...	...	0.28	...	...	0.052	0.07
$B_c^- \to D_s^- \bar{D}^{\star 0}$	0.225 (0.316)	...	...	6.3	...	...	1.3	1.9
$B_c^- \to D^{\star -} D^0$	1.595 (0.944)	40	7.9	49	18	30	8.8	12
$B_c^- \to D_s^{\star -} D^0$	0.315 (0.186)	2.38	0.55	4.5	0.91	1.8	0.65	0.7
$B_c^- \to D^{\star -} \bar{D}^0$	0.018 (0.027)	...	...	0.40	...	...	0.44	0.09
$B_c^- \to D_s^{\star -} \bar{D}^0$	0.418 (0.52)	...	...	8.5	...	...	9.3	2.5

39, 45 and 37%, respectively. This indicates that the interference is most significantly involved in $B_c^- \to D_s^-(\bar{D}^0, \bar{D}^{0\star})$ decays compared to other modes. This is, in particular, important since $B_c^- \to D_s^-(D^0, \bar{D}^0)$ decay modes have been proposed [54] for extracting the CKM angle γ through amplitude relations.

V. SUMMARY AND CONCLUSION

In this work we have studied the exclusive $B_c^- \to PP$, PV, VP decays within factorization approximation in the framework of the relativistic independent quark model based on the confining potential in equally mixed scalar-vector harmonic form. The weak decay form factors and their q^2 dependence are extracted in this model in the entire kinematical range. The predicted branching ratios are found in a wide range from minimum of $\mathcal{O}(10^{-6})$ for $B_c^- \to DD$ decays to maximum of 12.01% for $B_c^- \to \bar{B}_s^0\pi^-$. Summing up exclusive contributions, we find that the nonleptonic B_c transitions are dominated by $\bar{c} \to \bar{s}$, $\bar{d}$-induced modes contributing about 42%, the most promising of which are the CKM favored: $B_c^- \to \bar{B}_s^0\pi^-$, $B_c^- \to \bar{B}_s^0\rho^-$ and $B_c^- \to \bar{B}_s^{\star 0}\pi^-$ with branching ratios of 12.01, 9.97 and 8.61%, respectively, and should be accessible experimentally. The B_c meson, therefore, can be the source of B_s mesons as copious production of B_c mesons is expected at the Large Hadron Collider. On the other hand, the $b \to c$, u-induced modes were found to contribute less than 1% of the total decay rate against the estimated value of 20% [4], which leaves enough room for two-body nonleptonic B_c-meson decays to vector meson states, excited meson states and nonresonant multibody final states. The class-I decay modes determined by QCD coefficient a_1 are found to have comparatively large branching ratios, as expected, compared to that obtained for class-II decays determined by a_2. For class-III decays characterized by Pauli interference, the branching ratios are found to be too small $\sim\mathcal{O}(10^{-6})$ to be accessible experimentally. The analysis on effect of interference in these cases indicates that interference is most significantly involved in $B_c^- \to D_s^-(\bar{D}^0, \bar{D}^{0\star})$ decays compared to other modes. This is especially important since $B_c^- \to D_s^-(\bar{D}^0, \bar{D}^{0\star})$ decay modes have been proposed [54] for extracting the CKM angle through amplitude relations.

[1] F. Abe *et al.* (CDF Collaboration), Phys. Rev. D **58**, 112004 (1998); Phys. Rev. Lett. **81**, 2432 (1998).

[2] T. Aaltonen *et al.* (CDF Collaboration), Phys. Rev. Lett. **100**, 182002 (2008); A. Abulencia *et al.* (CDF Collaboration), Phys. Rev. Lett. **97**, 012002 (2006); **96**, 082002 (2006).

[3] V. M. Abazov *et al.* (D0 Collaboration), Phys. Rev. Lett. **101**, 012001 (2008).

[4] N. Brambilla *et al.* (Quarkonium Working Group), Report No. CERN-2005-005; M. P. Altarelli and F. Teubert, Int. J. Mod. Phys. A **23**, 5117 (2008).

[5] M. Wirbel, B. Stech, and M. Bauer, Z. Phys. C **29**, 637 (1985); M. Bauer, B. Stech, and M. Wirbel, Z. Phys. C **34**, 103 (1987); L.-L. Chau, H.-Y. Cheng, W. K. Sze, H. Yao, and B. Tseng, Phys. Rev. D **43**, 2176 (1991); **58**, 019902 (1998).

[6] I. P. Gouz, V. V. Kiselev, A. K. Likhoded, V. I. Romanovsky, and O. P. Yushchenko, Phys. At. Nucl. **67**, 1559 (2004).

[7] V. V. Kiselev, O. N. Pakhomova, and V. A. Saleev, J. Phys. G **28**, 595 (2002); V. V. Kiselev, arXiv:hep-ph/0211021; V. V. Kiselev, A. E. Kovalsky, and A. K. Likhoded, Phys. At. Nucl. **64**, 1860 (2001); Nucl. Phys. **B585**, 353 (2000).

[8] C. H. Chang and Y. Q. Chen, Phys. Rev. D **49**, 3399 (1994).

[9] M. A. Ivanov, J. G. Korner, and P. Santorelli, Phys. Rev. D **73**, 054024 (2006).

[10] D. Ebert, R. N. Faustov, and V. O. Galkin, Phys. Rev. D **68**, 094020 (2003); Eur. Phys. J. C **32**, 29 (2003).

[11] A. A. El-Hady, J. H. Munoz, and J. P. Vary, Phys. Rev. D **62**, 014019 (2000).

[12] A. Yu. Anisimov, I. M. Narodetskii, C. Semay, and B. Silvestre-Brac, Phys. Lett. B **452**, 129 (1999).

[13] P. Colangelo and F. DeFazio, Phys. Rev. D **61**, 034012 (2000).

[14] R. Dhir and R. C. Verma, Phys. Rev. D **79**, 034004 (2009); R. Dhir, N. Sharma, and R. C. Verma, J. Phys. G **35**, 085002 (2008).

[15] J. F. Liu and K. T. Chao, Phys. Rev. D **56**, 4133 (1997).

[16] Z. Rui, Z. Zhitian, and C.-D. Lu, arXiv:1203.2303v1.

[17] J. Sun, D. Du, and Y. Yang, Eur. Phys. J. C **60**, 107 (2009); J. Sun, Y. Yang, W. Du, and H. Ma, Phys. Rev. D **77**, 114004 (2008); J. Sun, G. Xue, Y. Yang, G. Lu, and D. Du, Phys. Rev. D **77**, 074013 (2008).

[18] X. Liu and X. Q. Li, Phys. Rev. D **77**, 096010 (2008).

[19] A. K. Giri, B. Mawlong, and R. Mohanta, Phys. Rev. D **75**, 097304 (2007); **76**, 099902(E) (2007).

[20] J. F. Cheng, D. S. Du, and C. D. Lu, Eur. Phys. J. C **45**, 711 (2006).

[21] S. Fajfer, J. F. Kamenik, and P. Singer, Phys. Rev. D **70**, 074022 (2004).

[22] G. L. Castro, H. B. Mayorga, and J. H. Munoz, J. Phys. G **28**, 2241 (2002).

[23] R. C. Verma and A. Sharma, Phys. Rev. D **65**, 114007 (2002); **64**, 114018 (2001).

[24] V. A. Saleev, Phys. At. Nucl. **64**, 2027 (2001); O. N. Pakhomova and V. A. Saleev, Phys. At. Nucl. **63**, 1999 (2000).

[25] R. Fleischer and D. Wyler, Phys. Rev. D **62**, 057503 (2000).
[26] L. B. Guo and D. S. Du, Chin. Phys. Lett. **18**, 498 (2001).
[27] Y. Dai and D.-S. Du, Eur. Phys. J. C **9**, 557 (1999).
[28] D.-S. Du and Z.-T. Wei, Eur. Phys. J. C **5**, 705 (1998).
[29] D. S. Du, G. R. Lu, and Y. D. Yang, Phys. Lett. B **387**, 187 (1996).
[30] A. V. Berezhnoy, V. V. Kiselev, A. K. Likhoded, and A. I. Onischenko, Phys. At. Nucl. **60**, 1729 (1997); S. S. Gershtein,V. V. Kiselev, A. K. Likhoded, A. V. Tkabladze, and A. I. Onishchenko, arXiv:hep-ph/9803433.
[31] V. V. Kiselev, arXiv:hep-ph/9605451.
[32] S. S. Gershtein, V. V. Kiselev, A. K. Likhoded, and A. V. Tkabladze, Phys. Usp. **38**, 1 (1995).
[33] Q. P. Xu and A. N. Kamal, Phys. Rev. D **46**, 3836 (1992).
[34] M. Masetti, Phys. Lett. B **286**, 160 (1992); D. S. Du and Z. Wang, Phys. Rev. D **39**, 1342 (1989).
[35] A. Rakitin and S. Koshkarev, Phys. Rev. D **81**, 014005 (2010); N. Sharma, Phys. Rev. D **81**, 014027 (2010); X. Liu and Z.-J. Xia, Phys. Rev. D **81**, 074017 (2010); D. Ebert, R. N. Faustov, and V. O. Galkin, Phys. Rev. D **82**, 034019 (2010); N. Sharma, R. Dhir, and R. C. Verma, J. Phys. G**37**, 075013 (2010).
[36] N. Barik, S. Naimuddin, P. C. Dash, and S. Kar, Phys. Rev. D **80**, 074005 (2009).
[37] N. Barik, B. K. Dash, and M. Das, Phys. Rev. D **32**, 1725 (1985); N. Barik and B. K. Dash, Phys. Rev. D **33**, 1925 (1986); **34**, 2092 (1986); **34**, 2803 (1986).
[38] N. Barik, B. K. Dash, and P. C. Dash, Pramana **29**, 543 (1987); N. Barik, S. Kar, and P. C. Dash, Pramana J. Phys. **48**, 985 (1997); N. Barik, S. Naimuddin, S. Kar, and P. C. Dash, Phys. Rev. D **59**, 037301 (1998).
[39] N. Barik, P. C. Dash, and A. R. Panda, Phys. Rev. D **46**, 3856 (1992); **49**, 299 (1994); Mod. Phys. Lett. A **10**, 103 (1995); N. Barik, S. Kar, and P. C. Dash, Phys. Rev. D **57**, 405 (1998); N. Barik, S. Naimuddin, S. Kar, and P. C. Dash, Phys. Rev. D **63**, 014024 (2000); N. Barik, P. C. Dash, and A. R. Panda, Phys. Rev. D **47**, 1001 (1993); N. Barik and P. C. Dash, Phys. Rev. D **47**, 2788 (1993); **53**, 1366 (1996); **56**, 4238 (1997); N. Barik, S. Naimuddin, P. C. Dash, and S. Kar, Phys. Rev. D **80**, 074005 (2009).
[40] N. Barik, S. Naimuddin, P. C. Dash, and S. Kar, Phys. Rev. D **77**, 014038 (2008); **78**, 114030 (2008); N. Barik, S. Naimuddin, and P. C. Dash, Int. J. Mod. Phys. A **24**, 2335 (2009).
[41] N. Barik, S. Kar, and P. C. Dash, Phys. Rev. D **63**, 114002 (2001); N. Barik, S. Naimuddin, P. C. Dash, and S. Kar, Phys. Rev. D **80**, 014004 (2009).
[42] J. D. Bjorken, in *Proceedings of the International Workshop, Crete, Greece, 1988*, edited by G. Branco and J. Romao, Developments in High Energy Physics [Nucl. Phys. B, Proc. Suppl. 11, 325 (1989)].
[43] A. J. Buras, J. M. Gerard, and R. Ruckl, Nucl. Phys. **B268**, 16 (1986).
[44] M. Neubert, Phys. Rep. **245**, 259 (1994).
[45] E. Hernandez, J Nieves, and J. M. Verde-velasco, Phys. Rev. D **74**, 074008 (2006).
[46] H.-M. Choi and C.-R. Ji, Phys. Rev. D **80**, 114003 (2009).
[47] M. Neubert and B. Stech, Adv. Ser. Dir. High Energy Phys. **17**, 294 (1998).
[48] M. Beneke, G. Buchalla, M. Neubert, and C. T. Sachrajda, Phys. Rev. Lett. **83**, 1914 (1999); **83**, 1914 (1999); Nucl. Phys. **B591**, 313 (2000); M. Beneke and M. Neubert, Nucl. Phys. **B675**, 333 (2003).
[49] C. E. Thomas, Phys. Rev. D **73**, 054016 (2006).
[50] J. Beringer *et al.* (Particle Data Group), Phys. Rev. D **86**, 010001 (2012).
[51] R. Dhir and R. C. Verma, Phys. Rev. D **79**, 034004 (2009); J. L. Rosner and S. Stone, arXiv:1201.2401v2 and references therein.
[52] T. E. Browder and K. Honscheid, Prog. Part. Nucl. Phys. **35**, 81 (1995); M. Neubert, V. Rieckert, B. Stech, and Q. P. Xu, in *Heavy Flavors* edited by A. J. Buras and H. Lindner (World Scientific, Singapore, 1992) and references therein.
[53] L. Wolfenstein, Phys. Rev. Lett. **51**, 1945 (1983).
[54] V. V. Kiselev, J. Phys. G **30**, 1445 (2004); R. Fleischer and D. Wyler, Phys. Rev. D **62**, 057503 (2000); M. Masetti, Phys. Lett. B **286**, 160 (1992); M. A. Ivanov, J. G. Korner, and O. N. Pakhomova, Phys. Lett. B **555**, 189 (2003).